SUPPLEMENTAL FIGURES

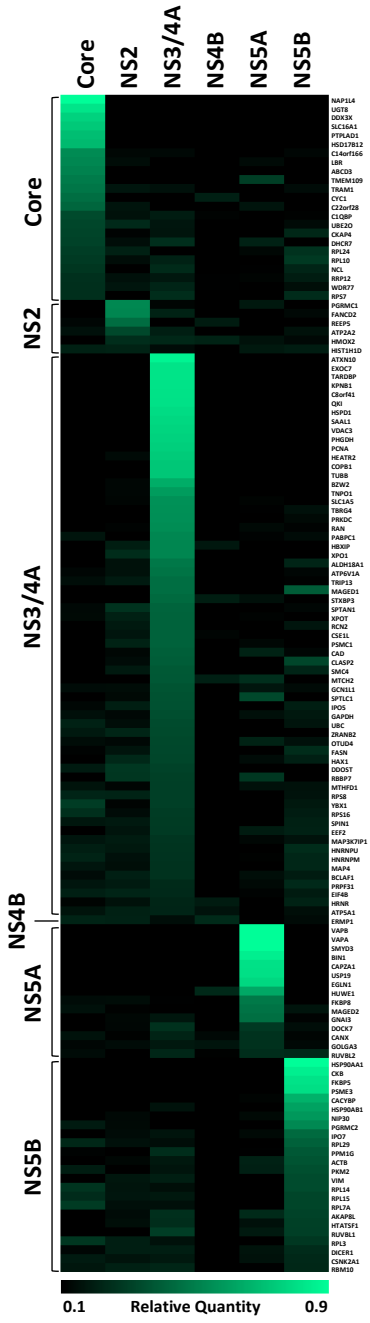

Figure S1. Host proteins specifically associated with HCV proteins.

Heat map visualization of the 132 host protein quantities significantly enriched in one of the six immunoprecipitations with HCV proteins 3XFLAG-Core, -NS2, -NS3/4A, -NS4B, -NS5A and -NS5B, modified from Germain *et al.* [1]. Proportions of presence for each of

the six experimental conditions are represented for host proteins hits (Σ six conditions = 1 for each host protein). The proteins are ordered from greatest to lowest proportion in their respective viral protein enrichment groups as determined by LC-MS/MS. The darker color correlates with the absence of the host protein in the condition, and brighter green indicates a high prevalence of the host protein in the condition (log_2 scale).

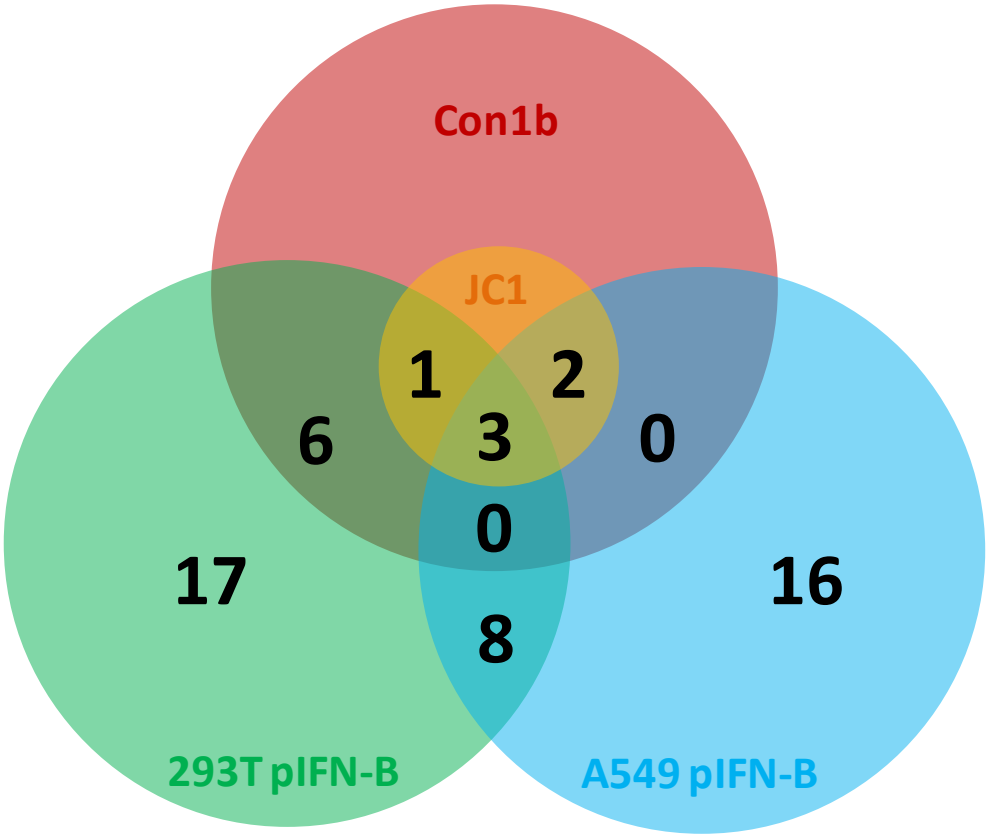

Figure S2. Venn diagram of HCV-host interactors modulating viral replication and IFNB1 production.

A Venn diagram representation of the effect of silencing 53 host interactors on IFNB1 production in comparison to their effect on HCV replication. Only 12 out of the 53 interactors met the stringent criteria of *Germain et al.* [1] for having a significant inhibitory effect on HCV replication, while the remainder interactors only affected the IFNB1 production upon SeV infection of HEK 293 or A549 cells.

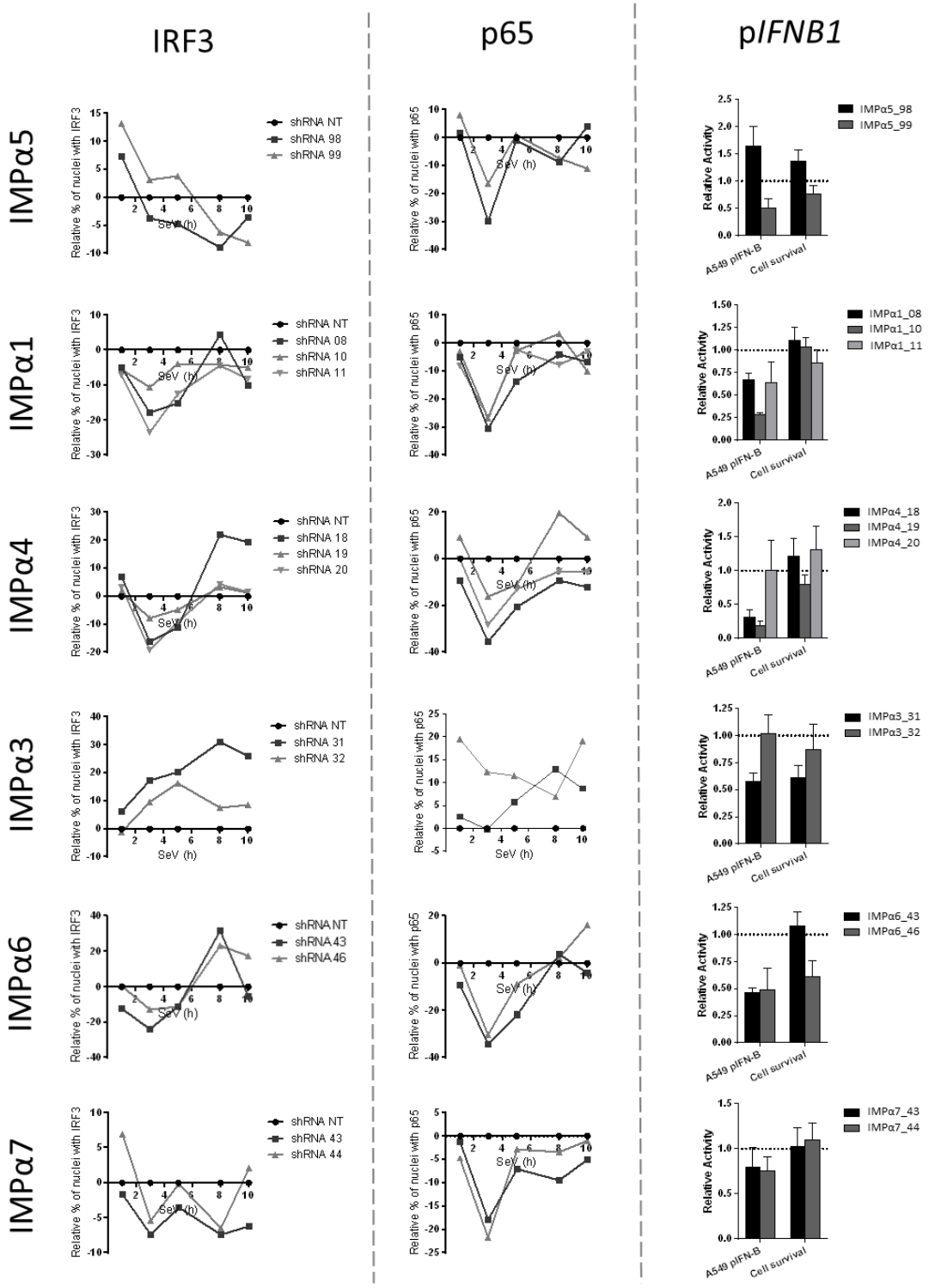

Figure S3. Effect of silencing IMP-α adaptors on IRF3 and p65 nuclear translocation.

The effects of IMP-α silencing are determined with the relative percentage of cells containing IRF3 and p65 in the nucleus after normalization of the control shRNA NT to

zero for all time points. Results are presented as individual shRNA for the 6 different IMP-α: IMPα1/KPNA2, IMPα3/KPNA4, IMPα4/KPNA3, IMPα5/KPNA1, IMPα6/ KPNA5, IMPα7/KPNA6. The effects of each shRNA-mediated knockdown on SeV-induced *IFNB1* production are measured in A549 cells stably expressing the firefly luciferase under the control of the *IFNB1* promoter, while the effects on cell proliferation and survival are evaluated using images from the microscopy screen by dividing the total number of nuclei for a given shRNA and dividing it by the total number of nuclei for the shRNA NT control.

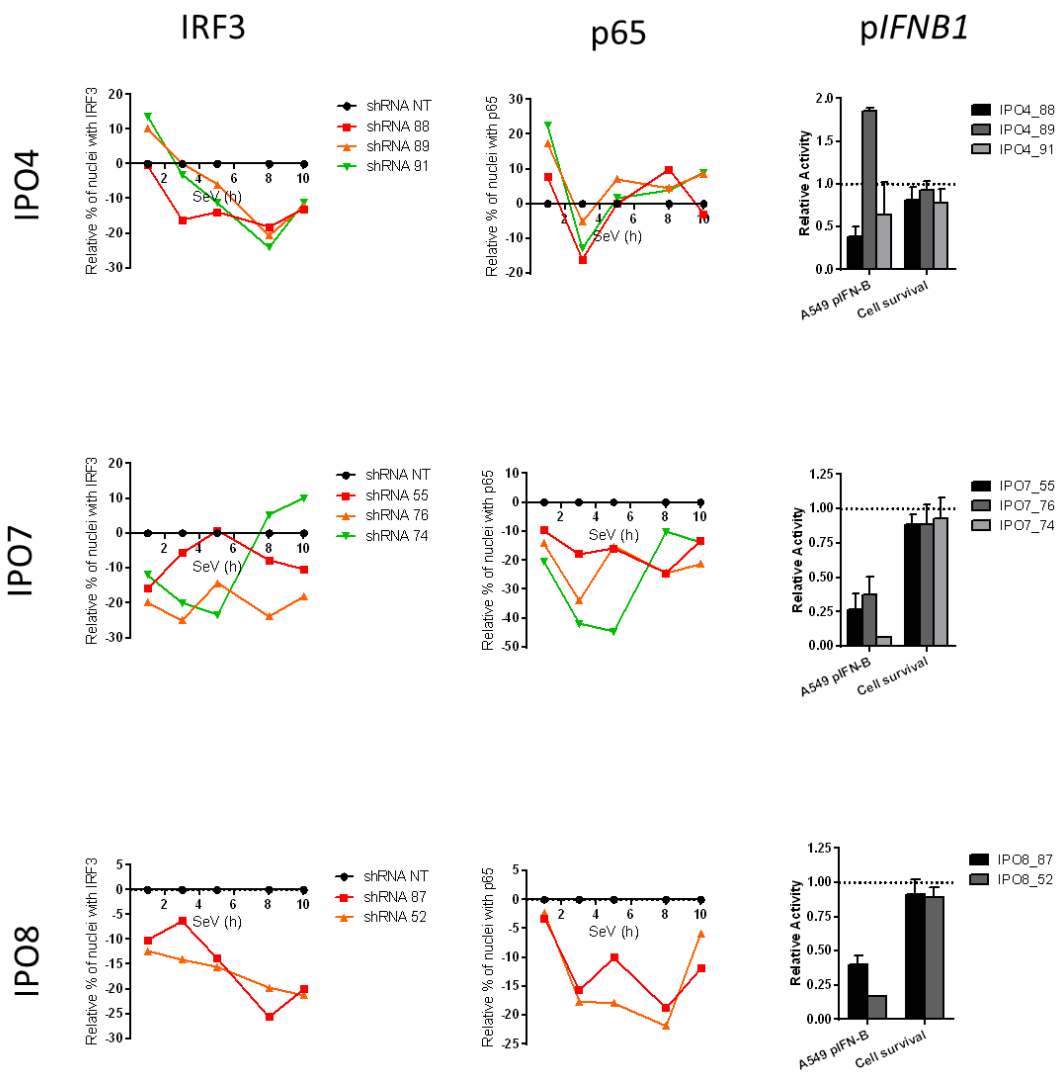

Figure S4. Effect of silencing importins on IRF3 and p65 nuclear translocation, p*IFNB1* induction and cellular fitness. The effects of IPO4, IPO7 and IPO8 silencing are determined with the relative percentage of nuclei with IRF3 and p65 staining, *IFNB1* promoter activity and cellular fitness, as described in Figure S3.

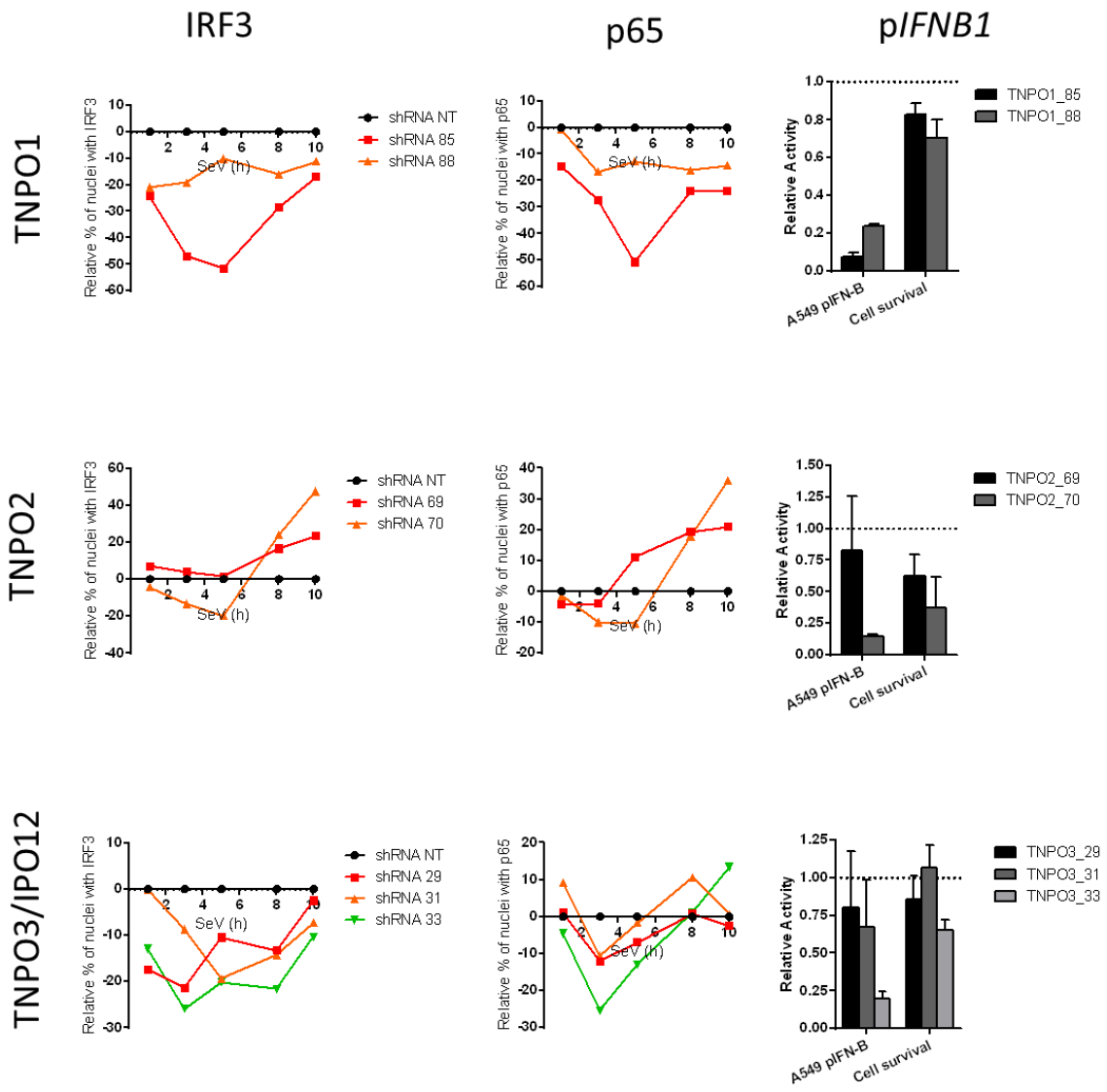

Figure S5. Effect of silencing transportins on IRF3 and p65 nuclear translocation, p*IFNB1* induction and cellular fitness. The effects of TNPO1, TNPO2 and TNPO3/IPO12 silencing are determined with the relative percentage of nuclei with IRF3 and p65 staining, *IFNB1* promoter activity and cellular fitness, as described in Figure S3.

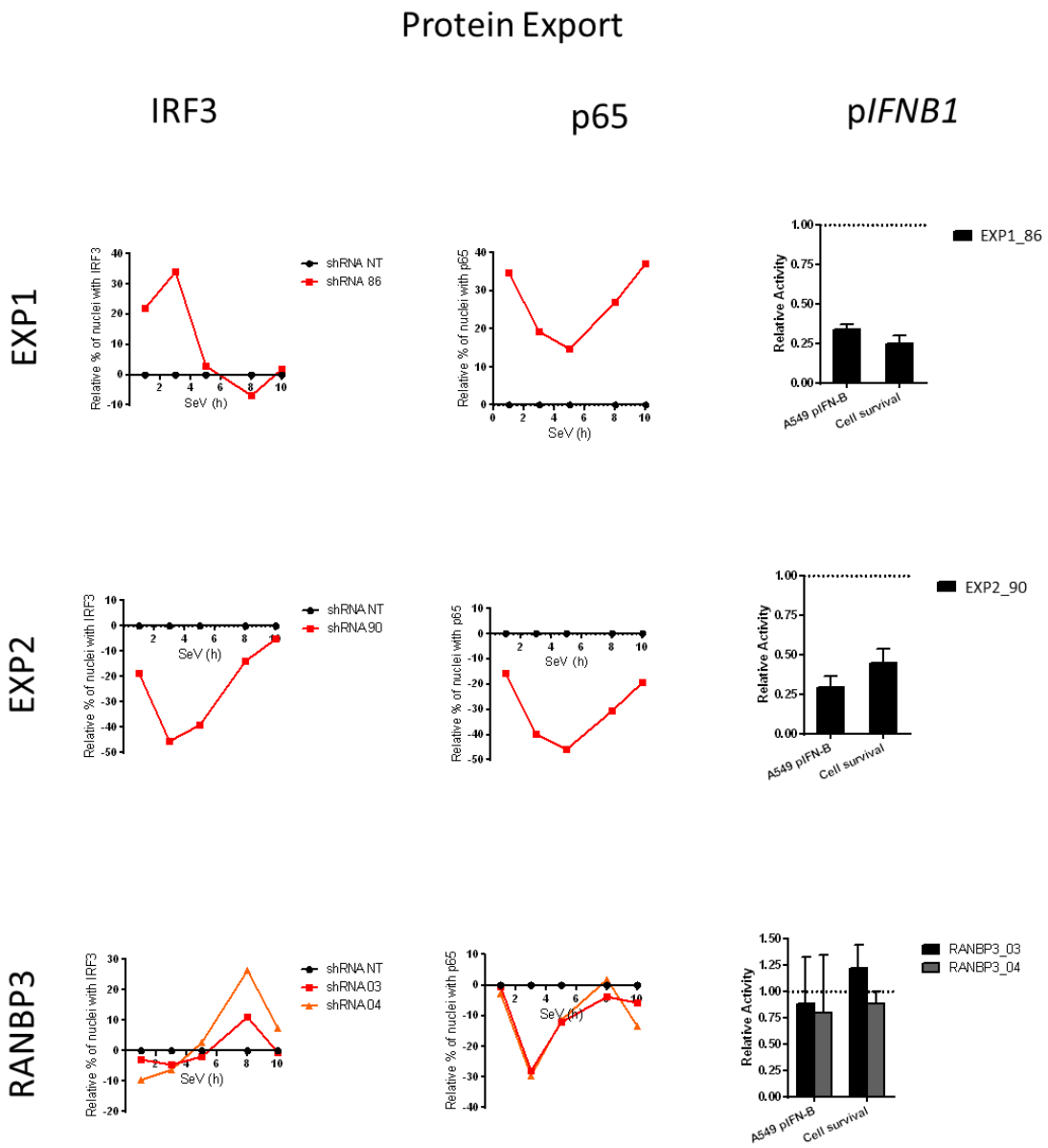

Figure S6. Effect of silencing proteins involved in protein export on IRF3 and p65 nuclear translocation, p*IFNB1* induction and cellular fitness. The effects of EXP/XPO1, EXP2/CSE1L and RANBP3 silencing are determined with the relative percentage of nuclei with IRF3 and p65 staining, *IFNB1* promoter activity and cellular fitness, as described in Figure S3.

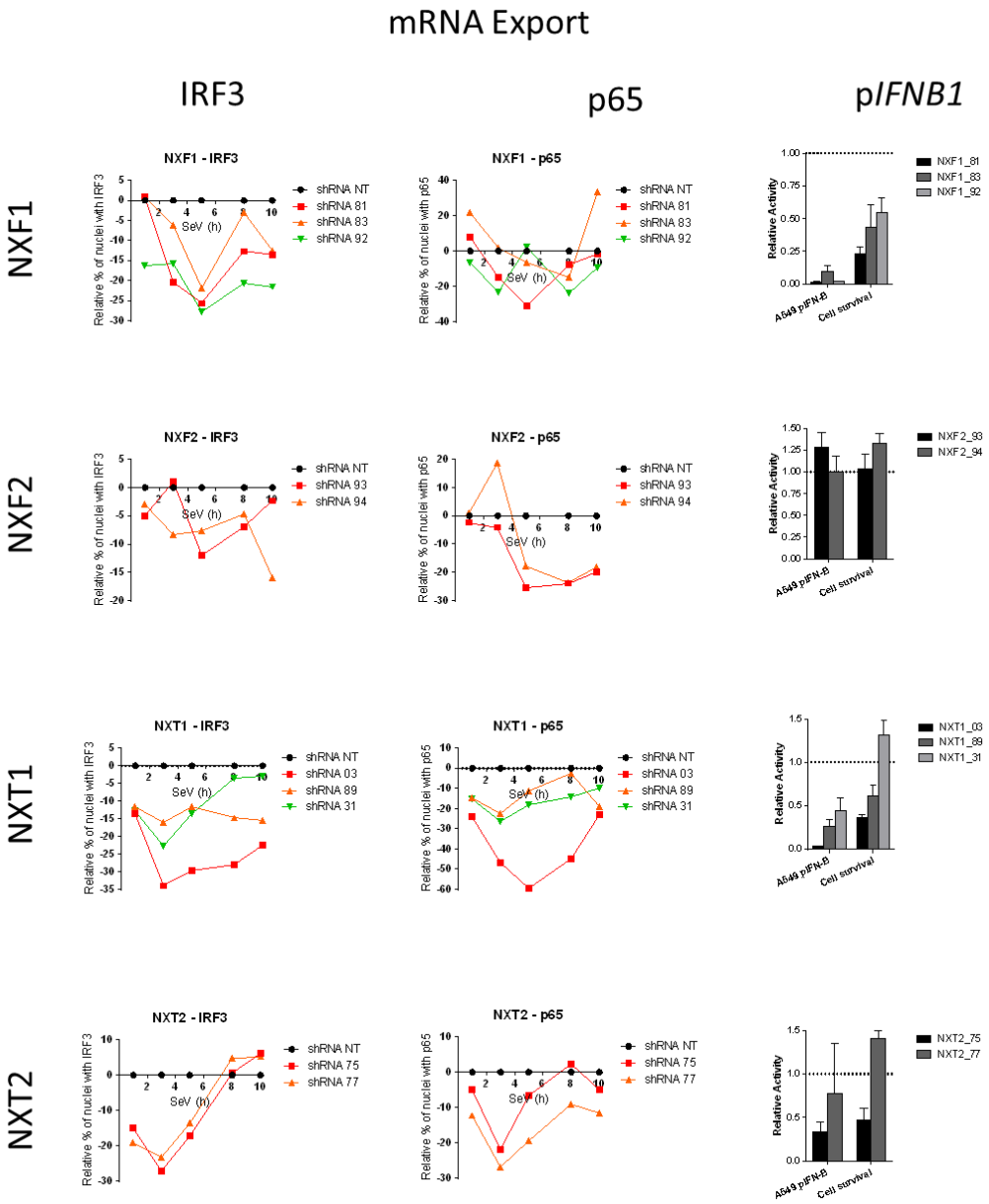

Figure S7. Effect of silencing proteins involved in mRNA export on IRF3 and p65 nuclear translocation, p*IFNB1* induction and cellular fitness. The effects of NXT1, NXT2, NXF1 and NXF2 silencing are determined with the relative percentage of nuclei with IRF3 and p65 staining, *IFNB1* promoter activity and cellular fitness, as described in Figure S3.

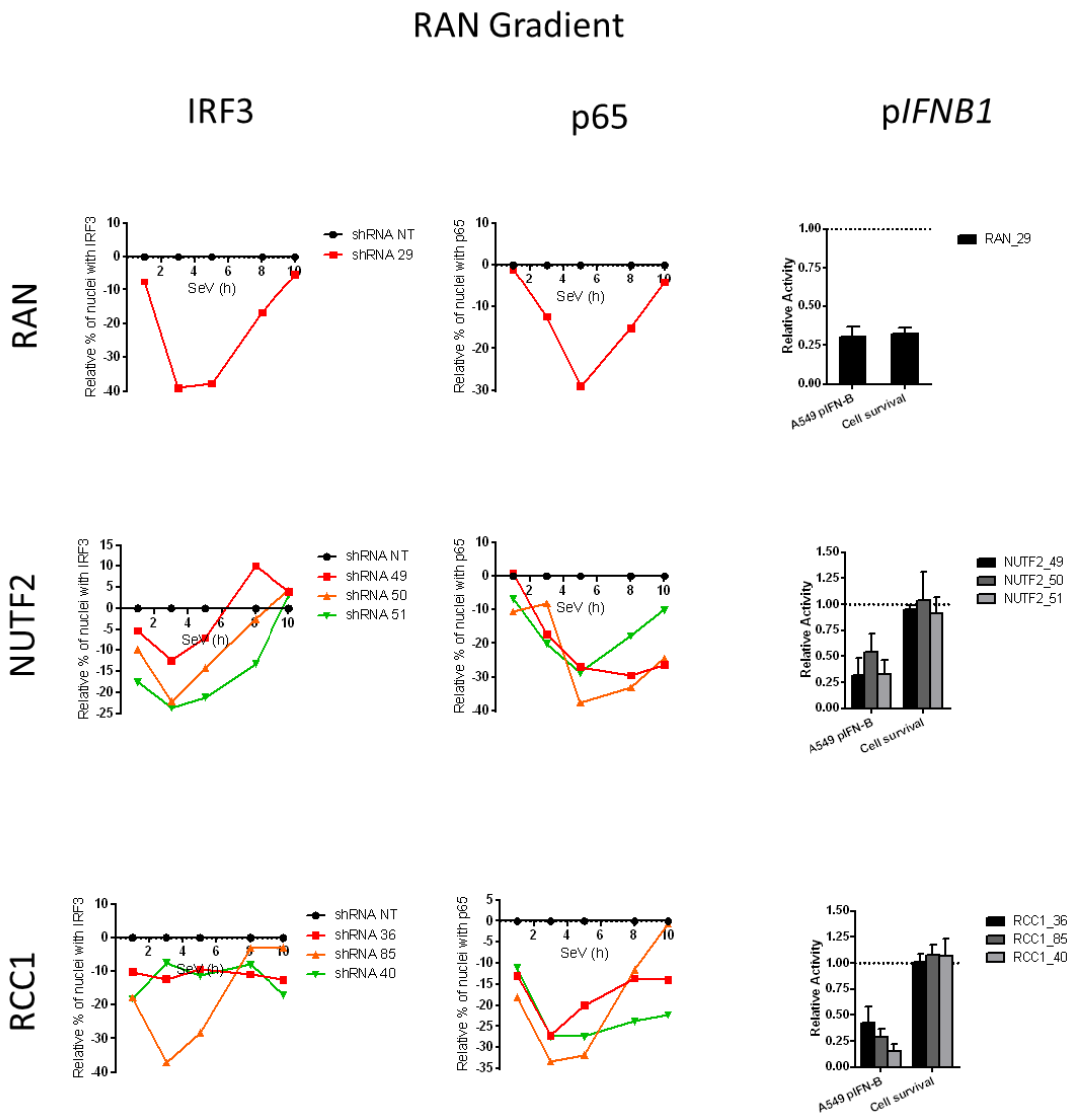

Figure S8. Effect of silencing proteins of the RAN system on IRF3 and p65 nuclear translocation, p*IFNB1* induction and cellular fitness. The effects of RAN, NUTF2 and RCC1 silencing are determined with the relative percentage of nuclei with IRF3 and p65 staining, *IFNB1* promoter activity and cellular fitness, as described in Figure S3.

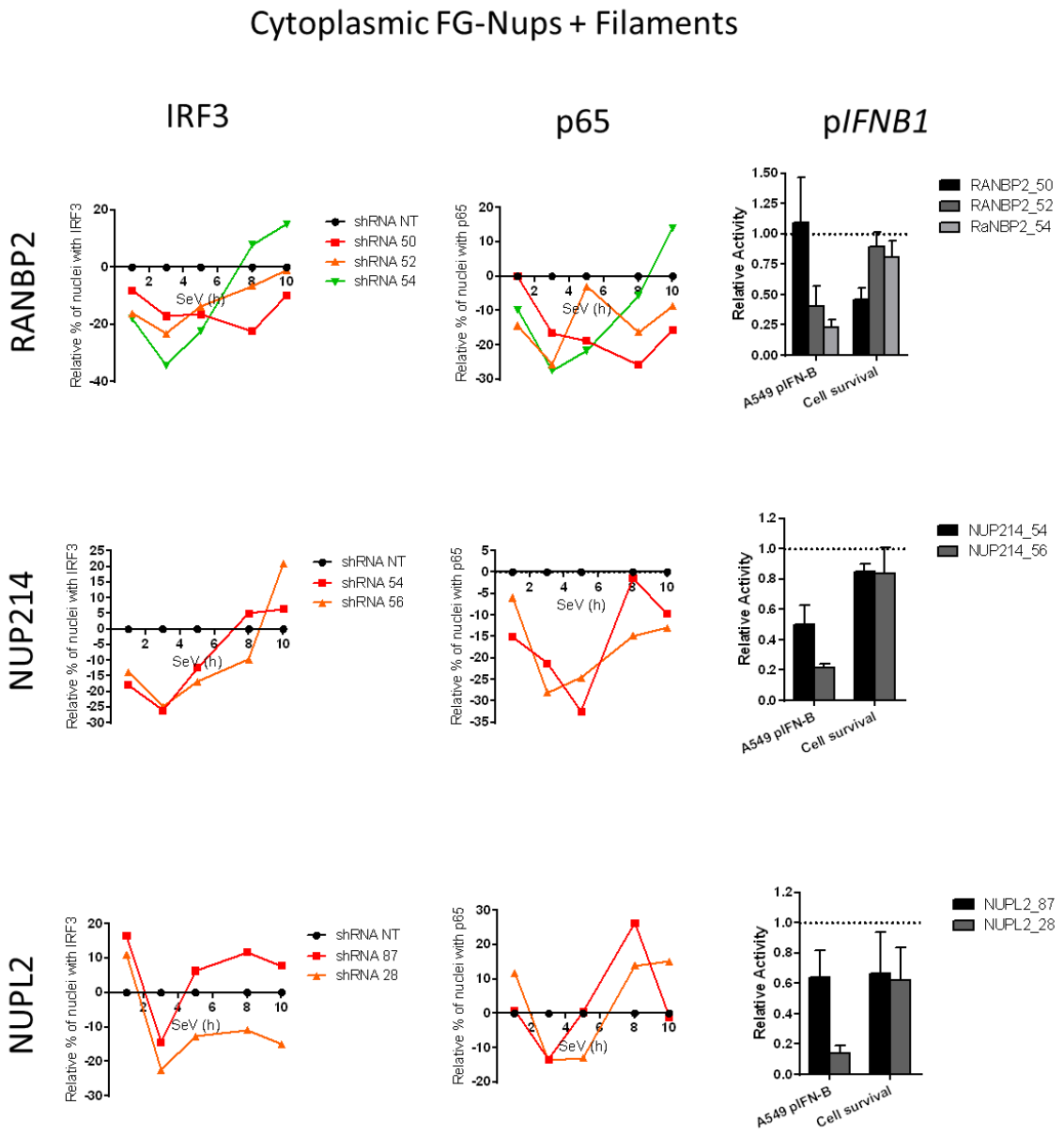

Figure S9. Effect of silencing cytoplasmic FG-Nups and filaments on IRF3 and p65 nuclear translocation, p*IFNB1* induction and cellular fitness. The effects of RANBP2, NUP214 and NUPL2 silencing are determined with the relative percentage of nuclei with IRF3 and p65 staining, *IFNB1* promoter activity and cellular fitness, as described in Figure S3.

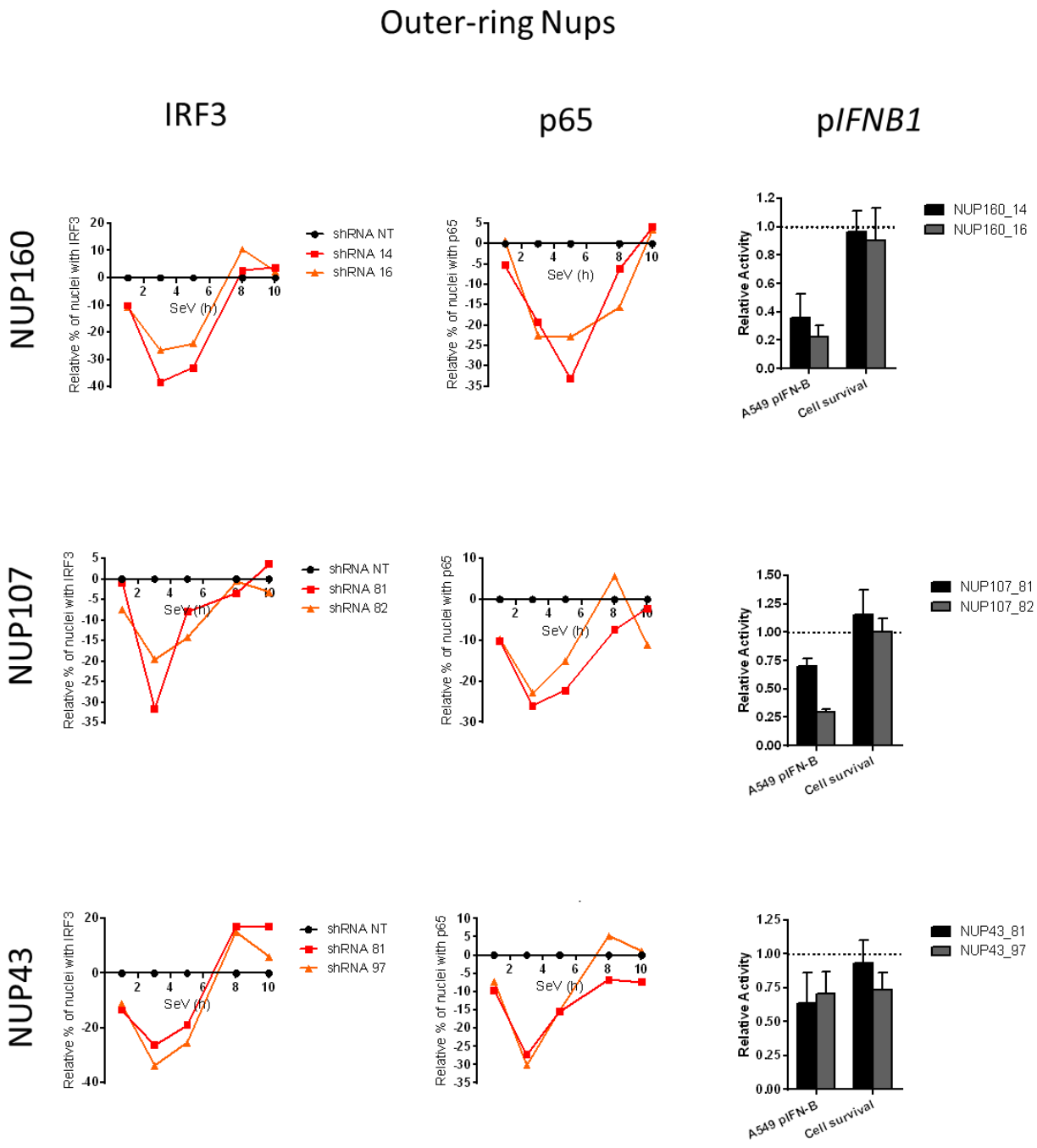

Figure S10. Effect of silencing outer-ring Nups on IRF3 and p65 nuclear translocation, p*IFNB1* induction and cellular fitness. The effects of NUP43, NUP107 and NUP160 silencing are determined with the relative percentage of nuclei with IRF3 and p65 staining, *IFNB1* promoter activity and cellular fitness, as described in Figure S3.

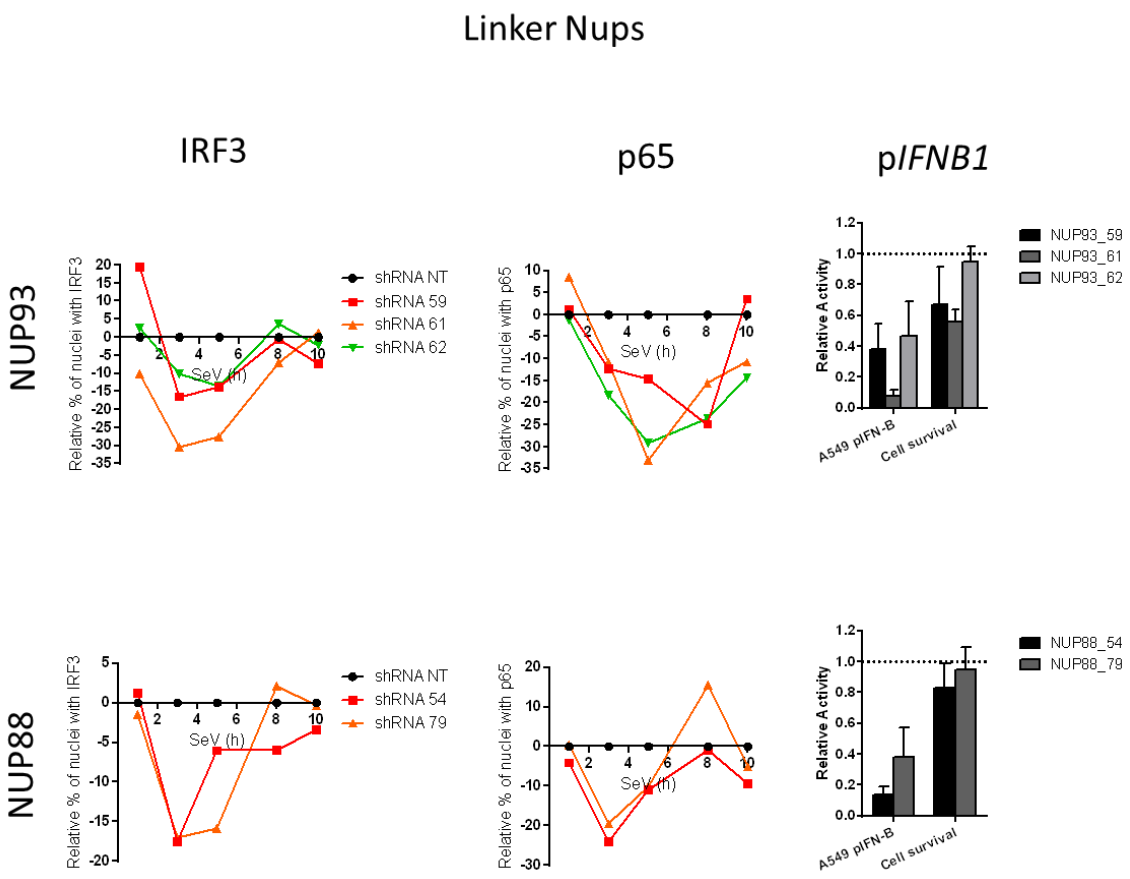

Figure S11. Effect of silencing linker Nups on IRF3 and p65 nuclear translocation, p*IFNB1* induction and cellular fitness. The effects of NUP93 and NUP88 silencing are determined with the relative percentage of nuclei with IRF3 and p65 staining, *IFNB1* promoter activity and cellular fitness, as described in Figure S3.

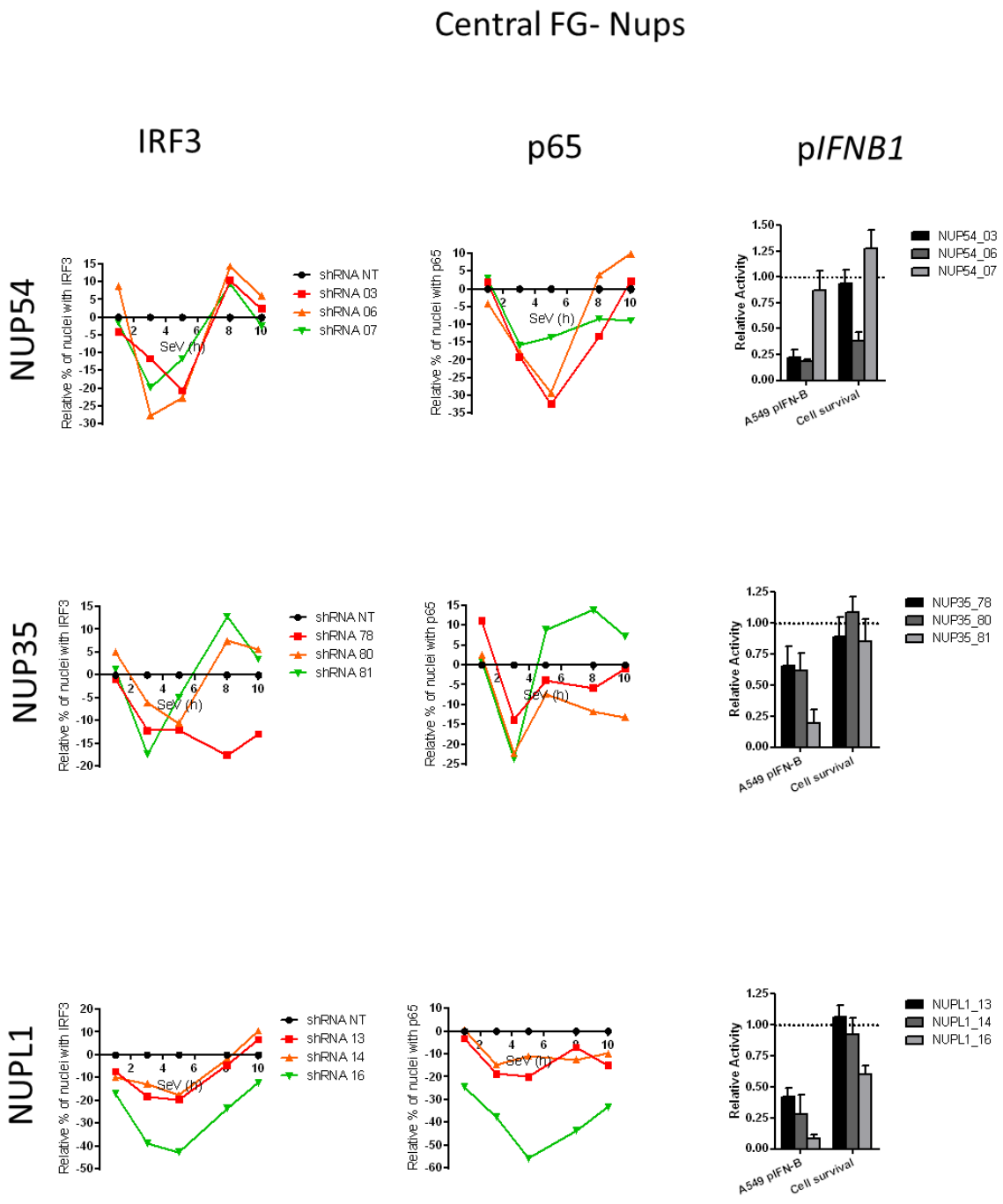

Figure S12. Effect of silencing central FG-Nups on IRF3 and p65 nuclear translocation, p*IFNB1* induction and cellular fitness. The effects of NUP54, NUP35 and NUPL1 silencing are determined with the relative percentage of nuclei with IRF3 and p65 staining, *IFNB1* promoter activity and cellular fitness, as described in Figure S3.

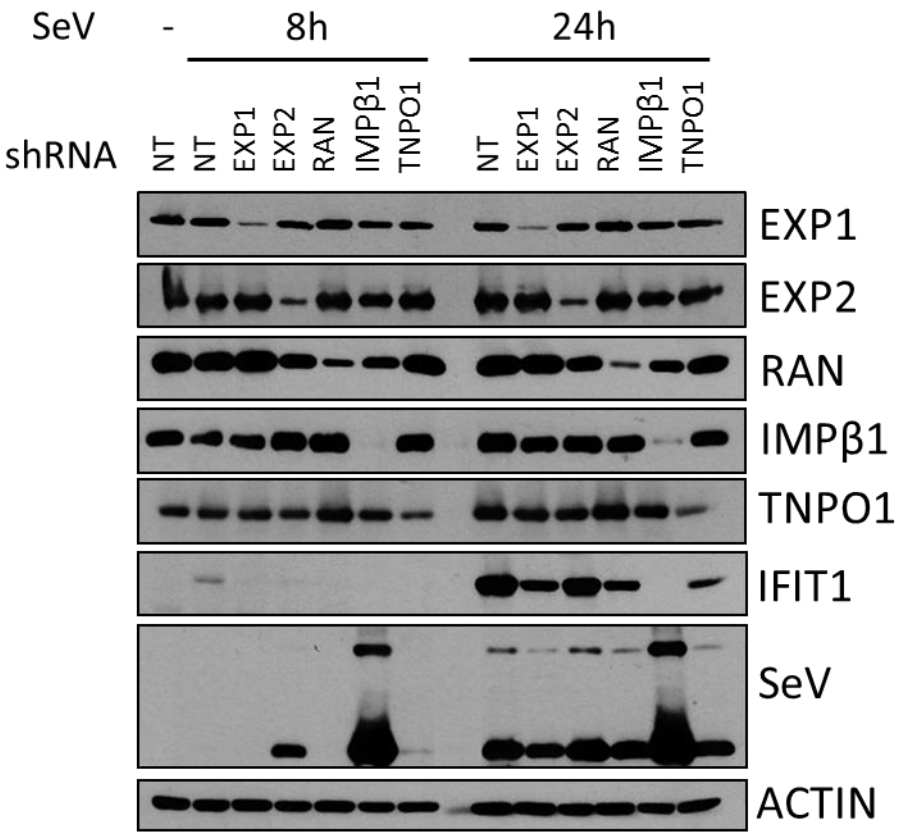

Figure S13. Effect of silencing expression of NS3/4A-interacting nuclear transport factors on SeV infection and IFIT1 induction. Immunoblot analysis of HEK 293T cells infected with SeV for 8 or 24 hours and transduced with lentivirus-encoding shRNA for three days to silence expression of EXP1/XPO1, EXP2/CSE1L, RAN, IMPβ1/KPNB1 and TNPO1/IMPβ2. shRNA NT is used as a control.

Table S1. Absolute and relative quantities of host protein interactions with each of the six HCV proteins. This table contains the results of the LC-MS/MS analysis with the absolute quantities, as well as the relative quantities of host proteins determined for the 6 viral protein conditions that are visually represented in Figure S1. This data is modified from *Germain et al.* [1].

Table S2. Effect of HCV-host interactors silencing on IFNB1 induction. This table contains the results of the gene silencing screen for 132 host interactors of HCV on SeV-mediated IFNB1 production. The average of 2 separate experiments is shown for HEK 293T and A549 cells. The non immune EF1α promoter-driven luciferase activities are used to prioritize genes selectively modulating *IFNB1* production and to identify shRNAs affecting basal transcription as well as for a measurement of cellular fitness.

Table S3. Effect of silencing nuclear transport factors on IRF3 and p65 nuclear translocation. This table contains the results of the gene silencing screen for 60 Nucleoporins, nucleocytoplasmic transporters or components of the RAN system on the nuclear translocation of IRF3 and NF-κB p65 during a 10-hour SeV infection time course. Non-target (NT) values are in absolute percentages, while all other values are presented in relative percentage.

Table S4. Effect of silencing nuclear transport factors on IFNB1 production and cellular fitness. This table contains the results of the gene silencing screen for 60 Nucleoporins, nucleocytoplasmic transporters or components of the RAN system on the

IFNB1 promoter-driven luciferase activity and cellular fitness. Results are represented in percentage of promoter inhibition from 2 separate experiments. Cellular fitness results are represented in percentage of cell survival for each time point of SeV infection.